COBEM 2023 27TH INTERNATIONAL CONGRESS OF MECHANICAL ENGINEERING

ABCM Brazilian Society of Mechanical Sciences and Engineering
27th ABCM International Congress of Mechanical Engineering
December 04-08, 2023, Florianópolis-SC, Brazil

COB-2023-2436
LAGRANGIAN COHERENT STRUCTURES IN NUMERICAL SIMULATIONS OF A FLUID MODEL OF TURBULENCE IN FUSION PLASMAS

Ana Luiza Piragibe Freire
Rodrigo Andrés Miranda Cerda
Sarah Gomes Da Silva Paes Da Costa
UnB-Gama Campus and Institute of Physics, University of Brasília (UnB), Brasília, DF, 72444-240, Brazil
alpiragibe@gmail.com, rmiracer@gmail.com, s.gspcosta@gmail.com

Abstract. *We perform numerical simulations of a fluid model that describes turbulence in fusion plasmas. By changing the value of a control parameter related to adiabaticity, the numerical solutions display a transition from a turbulent regime, into a regime dominated by zonal flows, in which turbulence and radial transport are suppressed. This transition can be regarded as a low-to-high (L-H) confinement transition, in which the low confinement regime is related to the turbulent regime, and the high-confinement regime is related to the zonal flow regime. The chaotic mixing properties of the flow are characterized by means of Lagrangian coherent structures (LCS). First, we compute the finite-time Lyapunov exponent (FTLE) of the calculated velocity field derived from the electrostatic potential to better characterize the chaotic mixing of the turbulent and zonal flow regimes. Then, we compare the statistics of the chaotic mixing of the two regimes using probability distribution functions (PDFs). These results can contribute to the understanding of turbulent transport processes in magnetic confinement fusion plasmas.*

Keywords: *turbulence, plasmas, finite-time Lyapunov exponent, Lagrangian coherent structures, chaotic mixing.*

1. INTRODUCTION

Due to global population growth and industrialization, the world's growing energy dependency has become a pressing concern. This concern revolves around our energy supply, as fossil fuels, a finite resource and significant contributor to climate change, emphasize the issue. Consequently, there is an escalating need for a clean, safe, and carbon-neutral form of electricity generation (Dewhurst, 2010). Nuclear fusion has gained recognition as an alternative solution for both energy dependency challenges and climate change.

Nuclear fusion occurs in the interior of stars. Fusion reactions, wherein nuclei fuse together, power the Sun, producing a mass that is smaller than the combined mass of the reactants. This small mass loss results into released energy (Dewhurst, 2010). There are ongoing efforts to reproduce fusion reaction in experimental facilities. In laboratory experiments, there are two main methods to recover the energy from fusion collision, namely, magnetic confinement and inertial fusion (Chen, 2016).

In magnetic confinement devices, a magnetic field is employed to take advantage of the forces acting on charged particles in plasmas for their confinement (Dewhurst, 2010). A plasma is an ionized gas or a quasineutral gas of charged and neutral particles exhibiting collective behavior (Chen, 2016), and serves as the required fuel for fusion to occur. The tokamak is a fusion reactor regarded as one of the most promising magnetic confinement devices to achieve energy production from thermonuclear fusion.

When investigating fusion plasma, turbulent processes pose a substantial engineering challenge, because they are responsible for the radial transport toward the edge of a tokamak, which leads to plasma loss to the walls (Farge *et al.*, 2006). A fundamental challenge of fusion research is to understand the dynamics of turbulent radial particle transport and heat flux in magnetized plasmas, because it holds the potential to enhance the confinement characteristics of fusion devices, including tokamaks (Bos *et al.*, 2008). Numerical simulations are a valuable tool to model this behavior, allowing the study of the overall plasma dynamics within the bulk region.

In this paper, we employ numerical simulations of a fluid model of turbulence in fusion plasmas that displays a low-to-high (L-H) confinement transition, which is a transition observed in experiments with fusion plasmas. Spontaneously occurring, these transitions occur as the plasma shifts from a low confinement regime, referred to as turbulent flow, to a turbulence-suppressed state characterized by the presence of zonal flows, resulting in a high confinement regime. The significance of this transition lies in its capacity to enhance confinement (Numata *et al.*, 2007), making the study of L-H transitions an avenue for advancing nuclear fusion.

Turbulence can be defined as the coexistence between advecting coherent structures and random fluctuations of the velocity fluid (Davidson, 2015). The detection of Lagrangian coherent structures (LCSs) in turbulent flows has received much attention since the last two decades (Haller, 2001, 2011; Beron-Vera *et al.*, 2010). Additionally, the computation of the finite-time Lyapunov exponent (FTLE) is employed for detecting Lagrangian coherent structures (LCS), thereby offering a more comprehensive characterization of the chaotic mixing during the L-H transition.

This paper is organized as follows. Section 2 describes the model employed and the numerical tools. Section 3 presents the numerical results, and Section 4 provides the conclusion.

2. COMPUTATIONAL METHODS

The following subsections discuss the numerical methods used in this paper.

2.1 The Hasegawa-Wakatani equations

The Hasegawa-Wakatani (HW) equations (Hasegawa and Wakatani, 1983; Wakatani and Hasegawa, 1984) describe, in a three-dimensional system setting, the resistive drift wave turbulence that occurs in magnetized plasma. These equations describe this phenomenon using the perturbations of plasma density (n) and electrostatic potential (φ). The HW equations can be written as (Numata *et al.*, 2007):

$$\frac{\partial}{\partial t}\zeta + \{\varphi, \zeta\} = \alpha\,(\varphi - n) - D\nabla^4\zeta, \tag{1}$$

$$\frac{\partial}{\partial t}n + \{\varphi, n\} = \alpha\,(\varphi - n) - \kappa\frac{\partial \varphi}{\partial y} - \nabla^4 n \tag{2}$$

where ζ is the vorticity, α is the adiabacity operator, and D is the dissipation coefficient. $\kappa \equiv (\partial/\,\partial x)\ln n_0$ is a constant that represents the background density. The term $\{a, b\} \equiv (\partial a/\partial x)(\partial b/\partial y) - (\partial a/\partial y)(\partial b/\partial x)$ represents the Poisson bracket (Numata *et al.*, 2007). The importance and relevancy of these parameters will be further explained in Section 2.2.

In the HW equations the α operator is responsible for making the system 3D. The approach taken in this paper is turning α into a parameter to establish a 2D system setting. The values of α are presented in Section 2.2. When the HW equations are restricted to such a setting it does not contain the zonal flow, however, Numata *et al.* (2007) presented an approach that permits the modification of the HW equations, allowing the capture of the zonal flow. This is done by subtracting the zonal components from the resistive coupling term $\alpha\,(\varphi - n)$ which turns it into $\alpha\,(\widetilde{\varphi} - \widetilde{n})$. The zonal and nonzonal components, respectively, of a variable f are defined as (Numata *et al.*, 2007):

$$\textbf{zonal}: \ \langle f \rangle = \frac{1}{L_y}\int f\,dy \tag{3}$$

$$\textbf{nonzonal}: \ \widetilde{f} = f - \ \langle f \rangle \tag{4}$$

where L_y is the length in y, and f stands for ζ and n (Numata *et al.*, 2007). This yields the modified HW equations presented in the next section.

2.2 Modified Hasegawa-Wakatani equations

The modified Hasegawa-Wakatani (MHW) equations represent a simplified model of the drift-wave turbulence in a tokamak plasma (Numata *et al.*, 2007)

$$\frac{\partial}{\partial t}\zeta + \{\varphi, \zeta\} = \alpha\,(\widetilde{\varphi} - \widetilde{n}) - D\nabla^4\zeta, \tag{5}$$

$$\frac{\partial}{\partial t}n + \{\varphi, n\} = \alpha\,(\widetilde{\varphi} - \widetilde{n}) - \kappa\frac{\partial \varphi}{\partial y} - \nabla^4 n \tag{6}$$

In this physical configuration, the model is situated within a tokamak plasma characterized by a constant magnetic field equilibrium $B = B_0\nabla z$, and a nonuniform density $n_0 = n_0(x)$ in the edge region. Within Equations (5) and (6), several parameters $\{a, b\}$ are utilized to represent the Poisson bracket, with n signifying the density fluctuations, and the ion vorticity $\zeta \equiv \nabla^2\varphi$ which is a 2D Laplacian depending on the electrostatic potential (φ). The background density $\kappa \equiv (\partial/\,\partial x)\ln n_0$ maintains an unvarying exponential profile and remains constant, while D represents the dissipation coefficient. In this physical setup, the adiabaticity operator α is assigned as a constant coefficient (Numata *et al.*, 2007). The velocity field equations are obtained from the electrostatic potential,

$$v_x \equiv -\frac{\partial \widetilde{\varphi}}{\partial y}, \tag{7}$$

$$v_y \equiv \frac{\partial \widetilde{\varphi}}{\partial x}. \tag{8}$$

The particle density flux Γ_r, is a correlation between the particle density (n) and radial velocity (v_r = -$\partial\widetilde{\varphi}$/ ∂y) (Bos *et al.*, 2008),

$$\Gamma_r = \langle n v_r \rangle . \tag{9}$$

In this model the radial direction is represented by the x direction, therefore $v_r \equiv v_x$, whereas the poloidal direction is represented by the y direction.

By changing the value of α and D, the MHW equations can display two different regimes, namely, a regime with turbulent patterns and formation of vortices, and a regime dominated by zonal flows Numata *et al.* (2007). We fix $D = 10^{-4}$ and $\kappa = 10^{-1}$, and set the α parameter to two different values, namely $\alpha = 0.0010$ and $\alpha = 0.0018$. The first value leads to numerical solutions with turbulent behavior (i.e., the low-confinement regime), whereas the second value leads to the zonal-flow regime (i.e., the high-confinement regime). We solve Eqs. (5)-(6) employing the finite differences method with a grid resolution of 256x256 for the spatial derivatives, and the 4th-order Runge-Kutta method for the time integration. The initial conditions are set to small-amplitude random fluctuations. Periodic boundary conditions are set for simplicity. The code is implemented it using a Fortran-90, and runs in parallel using the MPI protocol implemented by the MPICH library.

2.3 Finite-time Lyapunov exponents

The finite-time Lyapunov Exponents (FTLE) represent a useful tool to analyze the chaotic mixing properties of fluids. Subsequently, we observe the resulting Lagrangian coherent structures (LCS) that arise from the velocity field. These LCS can be defined as local maxima of the FTLE fields (Haller, 2001), representing special gradient lines that are transverse to the direction of minimum curvature (Shadden *et al.*, 2005).

The FTLE is defined as a finite time average of the maximum expansion rate for a pair of particles that are advected in the flow (Shadden *et al.*, 2005). Another definition characterizes the Lyapunov exponent as a measure of the sensitivity of a fluid particle's future behavior (Peacock and Haller, 2013). To define the FTLE mathematically, we must first consider the evolution of a perturbed point $\overrightarrow{x}' = \overrightarrow{x} + \delta\overrightarrow{x}$, where $\delta\overrightarrow{x}$ is infinitesimal and arbitrary oriented. After an interval τ, this perturbation becomes, $\delta\overrightarrow{x} = \overrightarrow{x}' - \overrightarrow{x}$,

$$\delta\overrightarrow{x}_\tau = \phi_{t_0}^{t_0+\tau}\left(\overrightarrow{x}'\right) - \phi_{t_0}^{t_0+\tau}\left(\overrightarrow{x}\right), \tag{10}$$

where the flow map is denoted as $\phi_{t_0}^{t_0+\tau}$, a map which takes a point in the domain at time t_0 to its location at time $t_0+\tau$, and can be expanded into a Taylor series in the neighborhood of $\overrightarrow{x}$,

$$\begin{aligned} \phi_{t_0}^{t_0+\tau}\left(\overrightarrow{x}'\right)\Big|_{\overrightarrow{x}} &= \phi_{t_0}^{t_0+\tau}\left(\overrightarrow{x}\right) + \left.\frac{d\phi_{t_0}^{t_0+\tau}}{d\overrightarrow{x}}\right|_{\overrightarrow{x}} \left(\overrightarrow{x}' - \overrightarrow{x}\right) + \dots \\ &\approx \phi_{t_0}^{t_0+\tau}\left(\overrightarrow{x}\right) + \left.\frac{d\phi_{t_0}^{t_0+\tau}}{d\overrightarrow{x}}\right|_{\overrightarrow{x}} \left(\overrightarrow{x}' - \overrightarrow{x}\right). \end{aligned} \tag{11}$$

The finite-time Cauchy-Green deformation tensor is defined as,

$$C_{t_0}^{t_0+\tau} = \left(\frac{d\phi_{t_0}^{t_0+\tau}}{d\overrightarrow{x}}\right)^T \left[\frac{d\phi_{t_0}^{t_0+\tau}}{d\overrightarrow{x}}\right]. \tag{12}$$

The eigenvectors of $C_{t_0}^{t_0+\tau}$ are denoted as $\overrightarrow{\xi}_1$ and $\overrightarrow{\xi}_2$, with corresponding eigenvalues $\lambda_1 > \lambda_2$ satisfying,

$$C_{t_0}^{t_0+\tau}\overrightarrow{\xi_i} = \lambda_i \overrightarrow{\xi}_i,\ i = 1,\ 2, \tag{13}$$

and $\left\|\overrightarrow{\xi}_i\right\| = 1$. In addition, it is supposed that the perturbation $\delta\overrightarrow{x}$ is aligned with $\overrightarrow{\xi}_1$ (being the maximum deformation),

$$\delta\overrightarrow{x}_0 = \|\delta\overrightarrow{x}_0\|\ \overrightarrow{\xi}_1. \tag{14}$$

From Equations (13) and (14),

$$\delta\overrightarrow{x}_\tau = \sqrt{\lambda_1}\ \|\delta\overrightarrow{x}_0\|. \tag{15}$$

Finally, the definition of the FTLE can be derived from Eq. (15) (Shadden *et al.*, 2005),

$$\sigma_{t_0}^{t_0+\tau}(\overrightarrow{x}) = \frac{1}{|\tau|} \ln \sqrt{\lambda_1}, \tag{16}$$

where the largest FTLE is given by Eq. (16) and can be computed for both positive and negative integration times (τ) due to the absolute value operation. The positive integration time is a forward-time integration that reveals a repelling LCS (Shadden *et al.*, 2005).

The FTLE is computed with a grid resolution of 1024x1024, and the results obtained are visualized and analyzed using Matlab. We also compute probability distribution functions (PDFs) of FTLE values with Matlab.

3. SIMULATION RESULTS

The following subsections display the results based on the previous numerical methods discussed in this paper.

3.1 Modified Hasegawa-Wakatani

A transition from L-H regimes in tokamaks can be modeled by varying the control parameter α in Eqs. (5)-(6). This transition can provide insight into the behavior of tokamak plasmas under different confinement conditions. Figure 1 depicts the 2D spatial patterns of the electrostatic potential ϕ obtained from numerical solutions of Eqs. (5)-(6) in two different regimes. The left panel of Figure 1 displays the patterns of ϕ in the turbulent regime, whereas the right panel of Figure 1 shows the patterns of ϕ in the zonal flow regime. The patterns were obtained by setting the value of the adiabaticity parameter α = 0.010 (turbulent regime) and α = 0.018 (zonal flow regime). Note that the color bars are set to the same scale, to facilitate the comparison between regimes. In this model, the left panel represents low confinement, while the right panel represents high confinement.

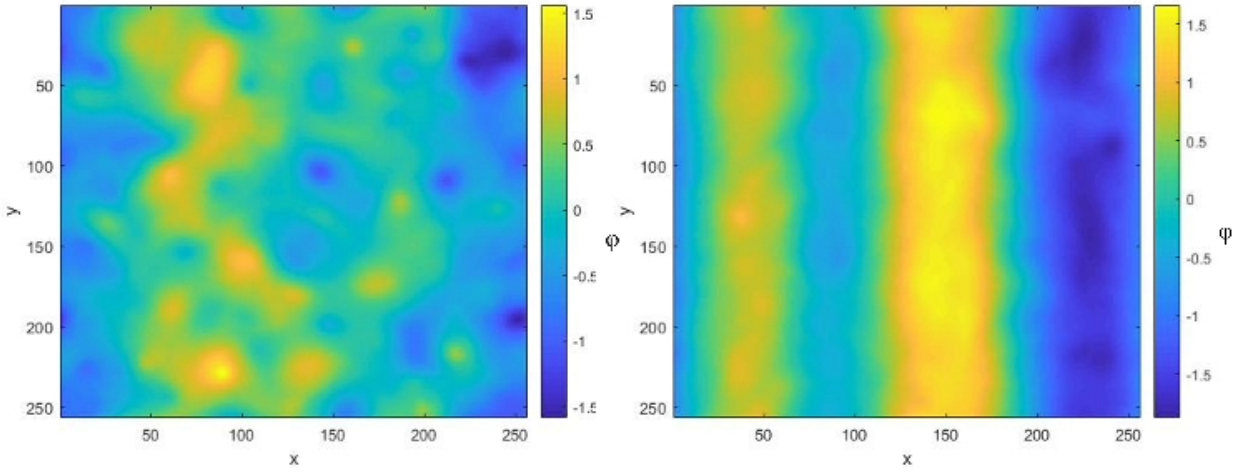

Figure 1. The electrostatic potential in the turbulent regime (left panel, α = 0.010) and zonal flow (right panel, α = 0.018).

The right-hand side of Figure 1 shows that ϕ displays zonally elongated structures visible as large-scale structures in the Y direction. These structures correspond to the zonal flows that emerge as a consequence of the Kelvin-Helmholtz instability of the drift waves, which effectively dampens drift wave activity (Numata *et al.*, 2007). Consequently, the zonal flow exhibits high confinement properties, rendering it a crucial element in comprehending plasma turbulence and confinement in tokamaks. Conversely, in the turbulent regime (left-hand side of Figure 1), ϕ displays a disordered pattern, which enhances drift wave activity and particle flow in the radial direction (i.e., the horizontal direction).

Table 1. Numerical values of Γ_r for the two regimes

Turbulent regime	1.4110
Zonal flow	-0.0758

Following Bos *et al.* (2008), we calculate the particle density flux Γ_r (Eq. (9)) of the turbulent and zonal flow regimes across the entire simulation domain. The computed values are shown in Table 1. These results show that the turbulent regime displays a higher Γ_r value compared to the zonal flow regime. This is expected since the elongated patterns of the

zonal flow act as transport barriers for the flow. This result emphasizes the importance of controlling turbulent flows for the confinement of plasma in a Tokamak.

Patterns of ϕ such as those shown in Figure 1 can offer clues about the presence of coherent structures. For instance, vortices can be associated with areas of localized minima and maxima of ϕ. These areas are readily discernible in the turbulent regime. Nonetheless, employing snapshots of fields (i.e., an Eulerian approach) for the detection of coherent structures such as vortices can yield misleading outcomes (Peacock and Haller, 2013). Coherent structures can be objectively identified using a Lagrangian approach, which will be applied in the next section.

3.2 Finite-time Lyapunov exponents

Figure 2 depicts the FTLE field $(\sigma_{t_0}^{t_0+\tau})$ obtained from the time-dependent velocity fields in the turbulent and the zonal flow regimes. The FTLE field was computed by setting $t_0 = 0$ and $\tau = 40\ \Omega_{ci}^{-1}$, where Ω_{ci} represent the ion cyclotron frequency, which is a fundamental time scale in plasmas. The value of τ must be obtained after some trial-and-error, checking the convergence of patterns of the FTLE field (Miranda *et al.*, 2013). Figure 2 offers a more detailed understanding of the spatiotemporal patterns of both the turbulent regime and the zonal flow regimes, for example, the locations of transport barriers within the flow. The numerical values of $(\sigma_{t_0}^{t_0+\tau})$ are represented using a color gradient, and fluid barriers can be identified in yellow. It becomes evident when comparing both panels of Figure 2 that these barriers seem to highlight locations of vortex structures in the turbulent regime (left panel), whereas in the zonal-flow regime there seems to be a fewer number of vortices.

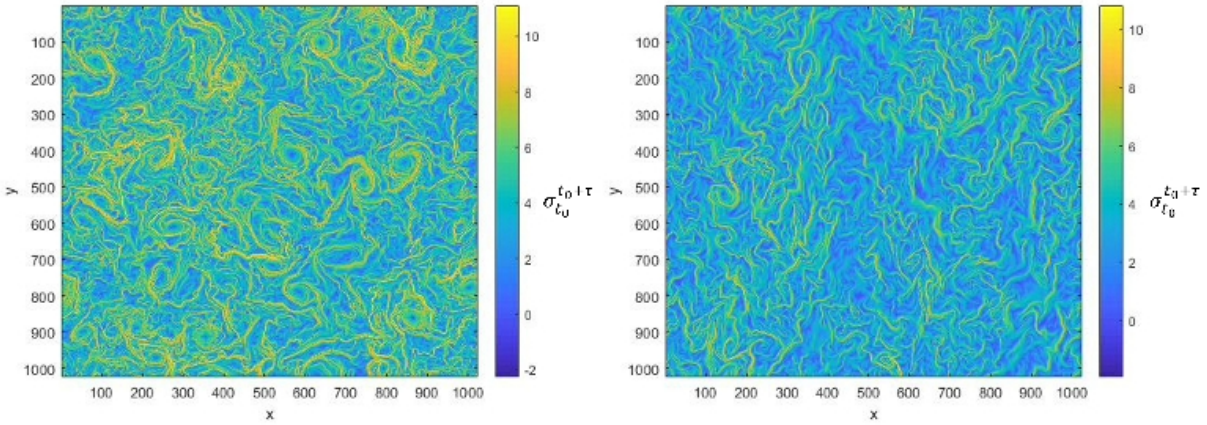

Figure 2. The finite-time Lyapunov exponent in the turbulent regime (left panel) and zonal flow (right panel).

The FTLE field provides a clear identification of coherent structures such as vortices, compared to an analysis based on an instantaneous snapshot such as those shown in Figure 1. For example, a comparison between Figures 1 and 2 reveals that not every localized maximum or minimum of ϕ from Figure 1 corresponds to a vortex. Moreover, the definition of vortex boundaries using instantaneous ϕ patterns can be a difficult task, and it is not certain that Eulerian vortices have a long duration. Lagrangian techniques such as the FTLE field allow to distinguish vortex boundaries by ridges of the FTLE field. This observation suggests that the FTLE is more effective at detecting vortices when compared to a visual inspection of the electrostatic potential.

The chaotic mixing properties of flows can be characterized from statistics of the FTLE field $(\sigma_{t_0}^{t_0+\tau})$. For example, the presence of broad PDFs can be linked to heterogeneous mixing (Beron-Vera *et al.*, 2010; Miranda *et al.*, 2013). The PDFs of the FTLE field depicted in Figure 2, are presented in Figure 3. From this figure, the PDF of the turbulent regime displays a broader shape compared to the PDF of the zonal flow regime. This result reveals that the turbulent regime exhibits a more heterogeneous mixing pattern than the zonal flow regime. The difference in mixing can be attributed to the fact that the zonal flow is a regime of high confinement that suppresses turbulent transport (Numata *et al.*, 2007), whereas the turbulent regime is characterized by the presence of vortices that propagate across the simulation domain, trapping plasma particles and transporting them in different directions, including the positive X direction, which in this model represents the radial direction towards the walls. Therefore, the PDFs displayed in Figure 3 represent an alternative technique to quantify chaotic mixing in turbulent flows.

4. CONCLUSION

In this paper we studied numerical simulations of the modified Hasegawa-Wakatani equations, in two different regimes, namely, a regime characterized by turbulent patterns, and a regime characterized by the presence of zonal flows. The chaotic mixing properties of the flow were elucidated by computing the finite-time Lyapunov exponents (FTLE), a com-

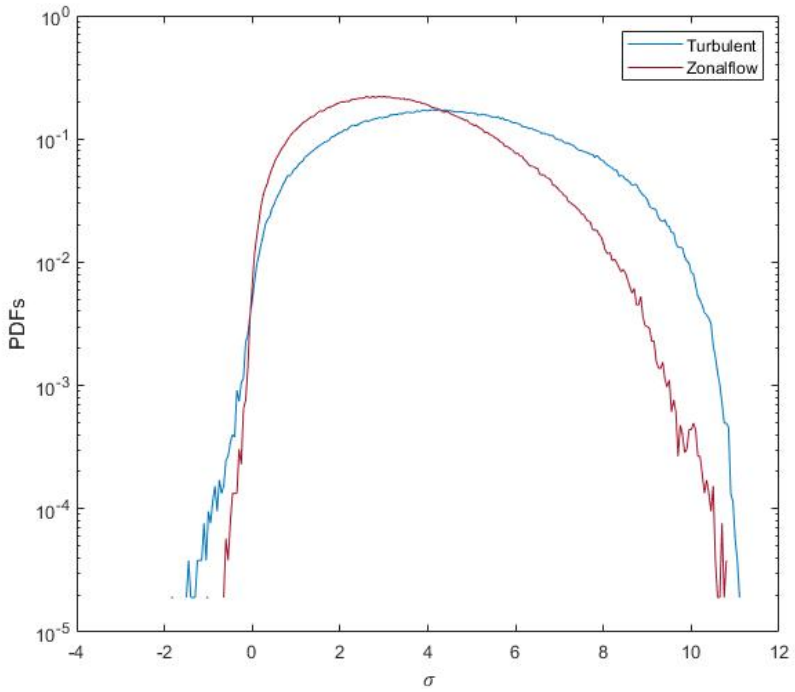

Figure 3. Probability distribution function of the finite-time Lyapunov exponent in the turbulent regime (blue line) and the zonal flow regime (red line).

monly used tool for Lagrangian analysis of turbulent fluids. By constructing probability distribution functions of the FTLE field and comparing their shapes, we demonstrated that the turbulent regime displayed a more heterogeneous mixing behavior than the zonal flow regime. This result is consistent with the high-confinement regime associated with the zonal flow, because zonal flows can suppress plasma transport in the radial direction. The radial transport is responsible for the loss of plasma particle to the walls of a tokamak (Farge *et al.*, 2006). The techniques and insights gained from our study may aid in the comprehension of drift-wave induced turbulence in tokamak plasmas.

The computation of the FTLE represents a simple technique for the detection of Lagrangian coherent structures based on ridges of the resulting field. However, we note that ridges of the FTLE field can lead to inconsistent results (Haller, 2011). Therefore, for future work, we are presently applying more advanced techniques such as geodesic theory (Haller and Beron-Vera, 2012). The techniques applied in this paper can be readily applied to turbulent flows that can arise in fluid mechanics, such as pipe flows, airfoils and aerodynamics. Therefore, Lagrangian techniques can enhance our understanding of turbulent flows in engineering.

5. ACKNOWLEDGEMENTS

ALP and SGSPC thank the Coordination for the Improvement of Higher Education Personnel (CAPES) for the financial support. RAM acknowledges support from CNPq (grants 407341/2022-6, 407493/2022-0) and COPEI/UnB (grant 7178).

6. REFERENCES

Beron-Vera, F.J., Olascoaga, M.J. and Goni, G.J., 2010. "Surface ocean mixing inferred from different multisatellite altimetry measurements". *Journal of Physical Oceanography*, Vol. 40, pp. 2466–2480.

Bos, W.J., Futatani, S., Benkadda, S., Farge, M. and Schneider, K., 2008. "The role of coherent vorticity in turbulent transport in resistive drift-wave turbulence". *Physics of Plasmas*, Vol. 15, p. 072305.

Chen, F.F., 2016. *Introduction to Plasma Physics and Controlled Fusion*. Springer International Publishing Switzerland, Los Angeles, CA, U.S.A.

Davidson, P.A., 2015. *Turbulence: an introduction for scientists and engineers*. Oxford University Press, Oxford, United Kingdom.

Dewhurst, J.M., 2010. *Statistical Description and Modelling of Fusion Plasma Edge Turbulence*. Ph.D. thesis, University of Warwick, England.

Farge, M., Schneider, K. and Devynck, P., 2006. "Extraction of coherent bursts from turbulent edge plasma in magnetic fusion devices using orthogonal wavelets". *Physics of Plasmas*, Vol. 13, p. 042304.

Haller, G., 2001. "Distinguished material surfaces and coherent structures in three-dimensional fluid flows". *Physica D: Nonlinear Phenomena*, Vol. 149, pp. 248–277.

Haller, G., 2011. "A variational theory of hyperbolic lagrangian coherent structures". *Physica D: Nonlinear Phenomena*, Vol. 240, pp. 574–598.

Haller, G. and Beron-Vera, F.J., 2012. "Geodesic theory of transport barriers in two-dimensional flows". *Physica D: Nonlinear Phenomena*, Vol. 241, pp. 1680–1702.

Hasegawa, A. and Wakatani, M., 1983. "Plasma edge turbulence". *Phys. Rev. Lett.*, Vol. 50, pp. 682–686.

Miranda, R.A., Rempel, E.L., Chian, A.C.L., Seehafer, N., Toledo, B.A. and Munoz, P.R., 2013. "Lagrangian coherent structures at the onset of hyperchaos in the two-dimensional navier-stokes equations". *Chaos: An Interdisciplinary Journal of Nonlinear Science*, Vol. 23, p. 033107.

Numata, R., Ball, R. and Dewar, R.L., 2007. "Bifurcation in electrostatic resistive drift wave turbulence". *Physics of Plasmas*, Vol. 14, p. 102312.

Peacock, T. and Haller, G., 2013. "Lagrangian coherent structures: The hidden skeleton of fluid flows". *Physics Today*, Vol. 66, pp. 41–47.

Shadden, S.C., Lekien, F. and Marsden, J.E., 2005. "Definition and properties of lagrangian coherent structures from finite-time lyapunov exponents in two-dimensional aperiodic flows". *Physica D: Nonlinear Phenomena*, Vol. 212, pp. 271–304.

Wakatani, M. and Hasegawa, A., 1984. "A collisional drift wave description of plasma edge turbulence". *Physics of Fluids*, Vol. 27, pp. 611–618.

7. RESPONSIBILITY NOTICE

The authors A L Piragibe, R A Miranda and S G S P Costa are solely responsible for the printed material included in this paper.